

Thermodynamic stability of Borophene, B_2O_3 and other $B_{1-x}O_x$ sheets

Florian M. Arnold^{1†}, Gotthard Seifert¹, Jens Kunstmann^{1† *}

keywords: 2D materials, borophene, B_2O_3 , B_2O , boron-oxygen, oxidation, phase diagram, convex hull

Abstract

The recent discovery of borophene, a two-dimensional allotrope of boron, raises many questions about its structure and its chemical and physical properties. Boron has a high chemical affinity to oxygen but little is known about the oxidation behaviour of borophene. Here we use first principles calculations to study the phase diagram of free-standing, two-dimensional $B_{1-x}O_x$ for compositions ranging from $x = 0$ to $x = 0.6$, which correspond to borophene and B_2O_3 sheets, respectively. Our results indicate that no stable compounds except borophene and B_2O_3 sheets exist. Intermediate compositions are heterogeneous mixtures of borophene and B_2O_3 . Other hypothetical crystals such as B_2O are unstable and some of them were found to undergo spontaneous disproportionation into borophene and B_2O_3 . It is also shown that oxidizing borophene inside the flakes is thermodynamically unfavorable over forming B_2O_3 at the edges. All findings can be rationalized by oxygen's preference of two-fold coordination which is incompatible with higher in-plane coordination numbers preferred by boron. These results agree well with recent experiments and pave the way to understand the process of oxidation of borophene and other two-dimensional materials.

Introduction

The investigation and development of two-dimensional (2D) materials is currently a focus of research worldwide [1, 2]. This class of materials was recently extended by another representative when two research teams were able to grow a boron monolayer on a silver surface in ultra-high vacuum [3, 4]. The experimental discovery of this "borophene" was anticipated by various theoretical predictions ranging back to the mid-1990s [5, 6, 7, 8]. Analogous to the existence of many boron bulk phases, free-standing borophene exhibits a pronounced polymorphism [7,

^{*1} Theoretical Chemistry, Department of Chemistry and Food Chemistry, TU Dresden, 01062 Dresden, Germany

§ Correspondence should be addressed to J.K. (e-mail: jens.kunstmann@tu-dresden.de) or F.M.A. (e-mail: florian.arnold@tu-dresden.de)

9]; however it is lifted in the vicinity of a metal surface which enables the growth of specific borophene crystals [10, 11]. A prototypical borophene (the α' -sheet) is shown in Fig. 1(a).

Boron is also known to have a high chemical affinity to oxygen and therefore boron-rich (nano)-structures can only be prepared under inert conditions or vacuum; so is borophene. For bulk phases the boron-oxygen system is well studied and several works on the phase diagram exist [12, 13, 14]. Thermodynamically stable are the pure "icosahedral" boron phases in their various forms [15], boron suboxide B_6O [16] and boron trioxide B_2O_3 that is a vitreous phase under ambient conditions [17] but can be crystalline when synthesized under pressure [18, 19, 14]. Sometimes boron monoxide B_2O [20, 21] is also considered but its stability and existence is strongly debated [22, 23, 12, 13]. However, as the bonding in borophene is different from the bonding in the bulk phases, we can expect it to have different chemical properties, which are largely unexplored so far. Feng *et al.* exposed borophene flakes to different oxygen concentrations and found that they tend to oxidize from the edges, while boron atoms inside the flakes are relatively inert to oxidation [4]. We will come back to this point in the discussion below. In the literature a variety of 2D boron-oxygen structures were studied. Two-dimensional variants of B_2O_3 were proposed by Ferlat *et al.* [17], with building blocks formed by planar BO_3 -units (see Fig. 1(b)) or boroxo-rings (see Supplementary Material). Similar B_2O_3 sheets were obtained as part of $A_3HB_4S_2O_{14}$ ($A=Rb, Cs$) crystals by Daub *et al.* [24]. Hexagonal B_2O is a (debated) layered van der Waals crystal [20] and multiple hypothetical structural models for monolayers were previously considered [25, 26]. One possible B_2O monolayer model is shown in Fig. 1(c). Several authors theoretically studied the adsorption of oxygen on the buckled triangular borophene [27, 28, 29, 30] or related nanoribbons [31]. However, structures related to the buckled triangular structure are not thermodynamically favorable neither as stand-alone system nor when placed on a metal surface [11] and angle-resolved photoemission spectroscopy of the experimentally realized borophenes (β_{12} and χ_3 sheets) are also highly consistent with non-triangular borophenes [32, 33]. A different theoretical study was performed by Luo *et al.* who considered oxygen adsorption, dissociation and diffusion on χ_3 borophene on Ag(111) [34]. They find that oxygen is not incorporated into the borophene layer (which mostly remains structurally intact) but it rather adsorbs on top of it. Sheets of varying composition, where oxygen is incorporated into the boron plane, were studied by Zhang *et al.* [35] and Lin *et al.* [36] considered B-O sheets that are inspired by the structure of planar B_2O_3 . Kambe *et al.* obtained a layered $B_{4.27}KO_3$ compound where planar, anionic B-O layers are stabilized by potassium cations between the layers [37].

To systematize and unify the view on these various structures we study 149 boron-oxygen layers by first principles calculations and use them to construct the convex hull of the 2D boron-oxygen system. The convex hull is related to the phase diagram and allows to decide which of these many systems are thermodynamically favorable and are likely to be realized experimentally. This also helps to understand the process of oxidation of borophene. Our findings shed a new light on the boron-oxygen binary system, put the previous literature into context and agree well

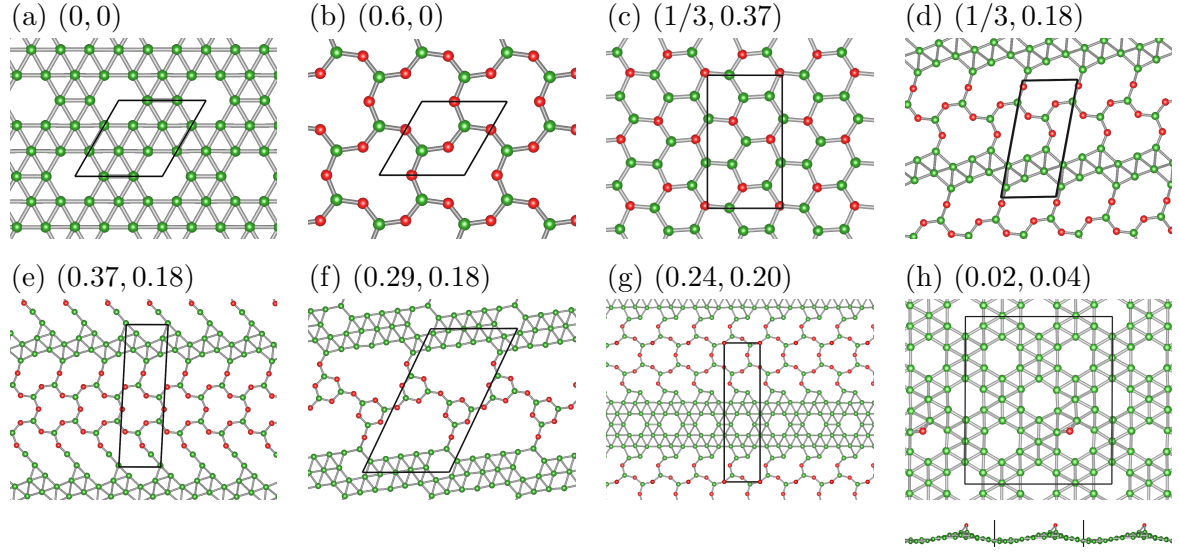


Figure 1: The structure of some two-dimensional $B_{1-x}O_x$ compounds. The tuples in the headlines correspond to (x, E_{mix}) , where x is the oxygen fraction and E_{mix} is the mixing energy in eV/atom (see Eqn. 1 and Fig. 2). Red and green balls represent oxygen and boron atoms, respectively. (a) Borophene α' -sheet. (b) B_2O_3 -sheet, introduced by Ferlat *et al.* [17]. (c) A B_2O -sheet with a honeycomb-like structure. (d)/(e) Systems that spontaneously separated into regions consisting of borophene and B_2O_3 during a structural optimization. (f)/(g) Larger systems that were constructed to be separated. (h) Oxygen on borophene, exhibiting divalent out-of-plane bonding, as discernible from the top view (top) and side view (bottom).

with experimental reports.

Computational methods

The first principles calculations of 2D $B_{1-x}O_x$ structures were performed with the density functional theory (DFT) code SIESTA, version 3.2 [38], using norm-conserving Troullier-Martins pseudopotentials [39] as provided on the SIESTA homepage as part of the Abinit's pseudo database. Electronic correlations were treated using the Perdew-Burke-Ernzerhof (PBE) exchange-correlation functional [40] within the generalized gradient approximation. Calculations were carried out using a default DZP basis set and an energy cutoff of 250 Ry for the real-space grid. The unit cells were built with 20 Å separation between replicas in the perpendicular direction to achieve negligible interactions. The k -space integrations were carried out using the Monkhorst-Pack scheme [41], employing a Fermi smearing of 300 K. The k -grids were converged for every considered structure such that energy changes were smaller than 1 meV/atom. Atomic coordinates as well as lattice parameters were relaxed using the conjugated gradient method with force tolerance 0.01 eV/Å and stress tolerance 0.1 GPa.

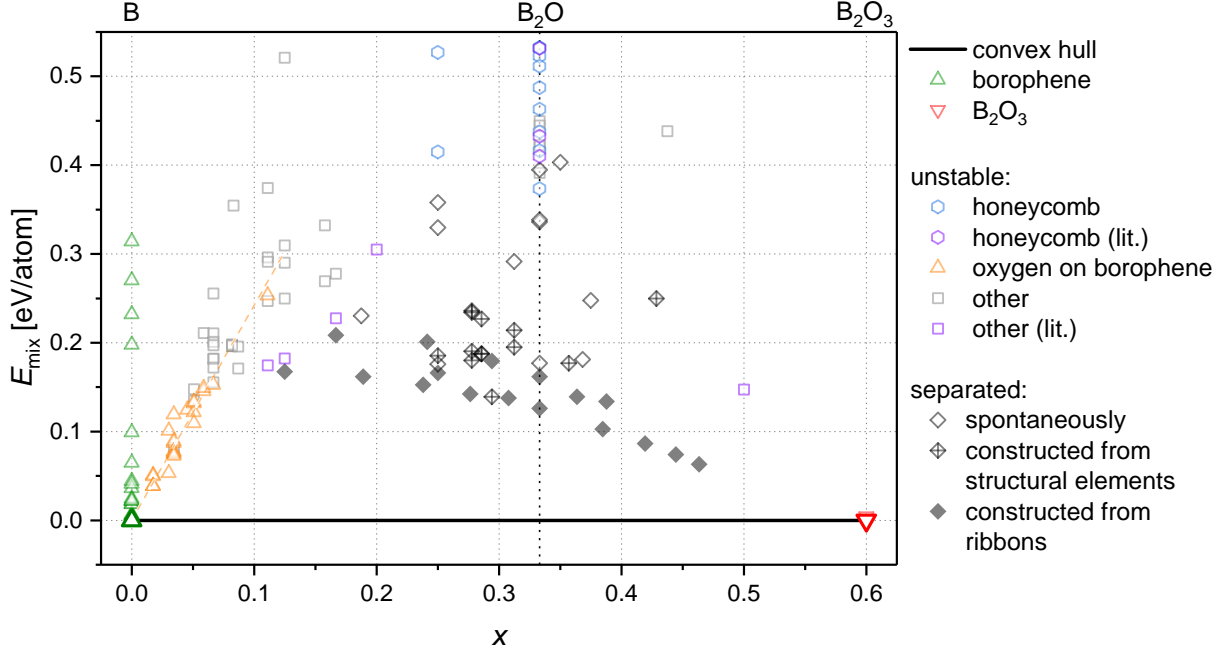


Figure 2: Scatter plot of mixing energies E_{mix} (see Eqn. 1) of free-standing, two-dimensional B_{1-x}O_x for different oxygen fractions x . The set of thermodynamically stable compounds in the diagram forms the convex hull. Here it is defined by the tie line connecting the borophene α' -sheet for $x = 0$ (see Fig. 1(a)) and a B_2O_3 sheet for $x = 0.6$ (see Fig. 1(b)). No other points are on the convex hull; consequently intermediate compositions are heterogeneous mixtures of borophene and B_2O_3 . Other data points with positive mixing energies represent thermodynamically unstable systems. These include decorations of the honeycomb-lattice (hexagons), oxygen on borophene (orange triangles), irregular structures (squares) and structures previously reported in the literature (purple symbols) [25, 35, 36]. Diamonds indicate heterogeneous mixtures of borophene and B_2O_3 in finite-size unit cells. Empty, gray diamonds indicate systems that spontaneously separated into borophene and B_2O_3 during a structural optimization run.

Results and Discussion

In order to construct the convex hull of free-standing, two-dimensional allotropes of boron and oxygen we considered a total number of 149 B_{1-x}O_x structures of varying composition x and symmetry. The geometry, energy and compositions of all systems are given in the Supplementary Material. To compare the different structures we define the mixing energy

$$E_{\text{mix}}(y) = E(\text{B}_{1-x}\text{O}_x) - (1 - y) \cdot E(\text{B}) - y \cdot E(\text{B}_2\text{O}_3) \quad (1)$$

where $E(a)$ is the DFT total energy per atom of structure a , $E(\text{B}) = -79.64$ eV/atom is the energy of the borophene α' -sheet [7, 8] and $E(\text{B}_2\text{O}_3) = -301.33$ eV/atom is the energy of a B_2O_3 sheet [17]. The relative oxygen fraction is given by $y = x/0.6$; this definition implies that

our maximum composition is $x = 0.6$ for B_2O_3 . The mixing energy E_{mix} can be considered as Gibbs free formation energy $G(x, p, T)$ at $p = 0$ Pa and $T = 0$ K for the fictitious reaction $(1 - y) \text{B} + y \text{B}_2\text{O}_3 \rightarrow \text{B}_{1-x}\text{O}_x$. The results are shown in the scatter plot in Fig. 2.

The borophene structures on the left-hand side of the plot (green triangles) are taken from various publications [4, 7, 6, 42, 8]. The rich polymorphism of boron is discernible by the large number of data points. In agreement with the literature we also find that (for the PBE functional) the α' -sheet (see Fig. 1(a)) is the lowest energy borophene for free-standing systems [7, 9]. It was therefore chosen as reference structure for calculating E_{mix} .

On the right-hand side of the figure (red triangles) we find another set of very stable structures - the B_2O_3 sheets proposed by Ferlat *et al.* [17]. Despite their different structure the two are nearly degenerate in energy. Figure 1(b) shows the B_2O_3 sheet with planar BO_3 -units that we use as second reference to define E_{mix} .

The hexagons for a composition of $x = 1/3$ in Fig. 2 correspond to crystalline B_2O structures. The initial structures were constructed using a honeycomb lattice (for details see Supplementary Material). We think this is a reasonable starting point as formally B_2O is isoelectronic to graphene [20]. We constructed 21 new structures of B_2O in addition to the three proposed by Zhang *et al.* [25] (indicated by purple hexagons). The honeycomb-like structure with the lowest mixing energy of 0.37 eV/atom is shown in Fig. 1(c). To our knowledge it was not reported before. However, all these honeycomb-like B_2O systems still have rather high, positive mixing energies, which indicates that they are thermodynamically unfavorable. Besides the many B_2O realizations on a honeycomb lattice we also find systems with rather irregular, non-hexagonal geometry (gray squares) and three structures with a particularly low energy (empty, gray diamonds). One of them is shown in Fig. 1(d) and its mixing energy is 0.18 eV/atom; much lower than the honeycomb-like structures. These three systems have an inhomogeneous distribution of boron and structurally transformed into regions of pure boron and regions consisting of boron and oxygen which exhibit BO_3 units, the typical structural unit of B_2O_3 . These findings suggest that B_2O is unstable with respect to spontaneous separation into boron and B_2O_3 as described by



This is a disproportionation reaction, in which B_2O (where B is in an intermediate oxidation state of +1) converts to two different compounds, borophen (with a lower oxidation state of 0) and B_2O_3 (with a higher oxidation state of +3). A chemically equivalent example is the reaction $3 \text{Al}_2\text{O} \rightarrow 4 \text{Al} + \text{Al}_2\text{O}_3$, which is discussed in textbooks [43]. As the disproportionation/separation of B_2O was found as a result of a simple structural optimization, it means that it occurs without energy barrier. This indicates that B_2O is not metastable (i.e. protected by energy barriers) but unstable. It should be mentioned that we only find such a separation if the distribution of oxygen and boron is inhomogeneous in the initial structures.

To further investigate the apparent tendency of honeycomb-like B-O to disproportionate into

heterogeneous mixtures of borophene and B_2O_3 , we extended the study to a broader stoichiometric range. Structures were again constructed by placing atoms on the sites of a honeycomb lattice, but now the B:O ratio was varied and boron and oxygen were deliberately distributed inhomogeneously. During the geometry optimization some of the systems remained honeycomb-like (hexagons in Fig. 2), some transformed into irregular structures (squares), but most of the systems spontaneously separated into borophene and B_2O_3 (empty diamonds). An example of the last category is shown in Fig. 1(e), which corresponds to $x = 0.37$ and $E_{\text{mix}} = 0.18$ eV/atom. The strong structural changes that are associated with the disproportionation are illustrated in the Supplementary Material, where all initial and final structures are given. Thus spontaneous disproportionation/separation occurs over a broad stoichiometric range and separated systems tend to have low mixing energies. This is a very strong hint that the corresponding layered B_2O bulk phase, reported by Hall *et al.* [20], is unlikely to exist, as well. Our findings are also in good agreement with those of Grumbach *et al.* [22], who found hints for disproportionation in diamond-like B_2O [21], very similar to the one described here. From this point of view, our results can be seen as a possible explanation why there are no conclusive reports about the existence of bulk B_2O [23, 12, 13].

To lower E_{mix} further, structures that are already separated in their initial geometry were studied. The typical structural elements used for this approach were triangular units for boron and BO_3 -units and boroxo-rings for B_2O_3 . These were connected to form areas of pure boron linked to areas of B_2O_3 . An example from this set of structures is shown in Fig. 1(f). The energies are shown as crossed, gray diamonds in Fig. 2. It is obvious that E_{mix} is significantly lower for such systems. The last approach to construct separated systems was by using boron and B_2O_3 ribbons (for details see the Supplementary Material). An example for these structures is shown in Fig. 1(g). These structures show the overall lowest mixing energies of all studied sheets (filled, gray diamonds in Fig. 2). We also added the energy of the structures studied by Zhang *et al.* [35] and Lin *et al.* [36] to Fig. 2 (purple symbols). Their mixing energy is significantly higher than the ones of the heterogeneous mixtures, indicating that they are thermodynamically unfavorable. All the described approaches yield the same result for the considered range of compositions - the lowest energy structures are heterogeneous mixtures of borophene and B_2O_3 .

To generate systems with small oxygen fractions 50 structures were constructed by adding oxygen atoms to different borophene sheets ($\alpha, \alpha_1, \beta, \beta_1, \chi_3$ following the notation by Wu *et al.* [8]). We found that for $x < 0.05$ (orange triangles in Fig. 2) the systems are mostly characterized by divalent oxygen atoms binding out-of-plane to sites near the hexagonal holes of the borophene sheets. The sheets themselves remain intact and are structurally modified only in the vicinity of the O atom. Figure 1(h) shows one example of such a system. These findings agree well with similar results by Luo *et al.* [34]. For $x \geq 0.05$ oxygen tends to be incorporated in-plane and the structure is distorted (indicated by squares in Fig. 2). The data points in Fig. 2 for small x rise linearly and the slope ($\mu_o = 2.53$ eV/atom) is the chemical

potential. Mind that μ_o is defined relative to borophene and B_2O_3 . So the positive value means that oxidizing borophene inside the flakes is thermodynamically unfavorable over forming heterogeneous mixtures of borophene and B_2O_3 . This is in full agreement with the experimental observation by Feng *et al.*, who found that borophene flakes tend to oxidize from the edges (forming B_2O_3), while boron atoms inside the flakes are relatively inert to oxidation [4]. Further support for these results comes from our finding that the edge energy of a B_2O_3 ribbon is only 0.25 eV per edge atom, while the edge energy of a borophene ribbon is 1.62 eV/atom, i.e., more than 6 times bigger (see Supplementary Material). We can assume that the edge energy of a flake is similar to the one of a ribbon. Then the oxidation of a borophene flake from the edges (by forming B_2O_3) not only allows the system to minimize the mixing energy, that represents the bulk of the flake, but also to reduce the edge energy.

From a chemical point of view all our results are easy to explain. In honeycomb-like B_2O -structures oxygen atoms are 3-fold coordinated, incorporated into borophene layers, oxygen would be 6-fold coordinated. However it is a well-known fact that oxygen prefers coordination numbers lower than 3 and this is only possible in B_2O_3 , where its coordination number is two. And indeed strong structural reorganisations, leading to the formation of B_2O_3 areas, are mostly observed for systems where oxygen is over-coordinated in the initial structure.

Considering all data points in Fig. 2, we are now in the position to determine the convex hull. It is defined by the set of thermodynamically stable compounds. For the 2D $B_{1-x}O_x$ binary system and compositions $0 \leq x \leq 0.6$ the convex hull is equivalent to the tie line connecting the borophene α' -sheet for $x = 0$ and the B_2O_3 sheet for $x = 0.6$. No other points are on the convex hull and the structures with positive mixing energies represent thermodynamically unstable systems, which include honeycomb-like B_2O [20, 25] or other previously considered structures [26, 35, 36]. The gray diamonds in Fig. 2 lie above the convex hull. They represent heterogeneous mixtures of borophene and B_2O_3 in finite size unit cells. In these cells relatively small areas of borophene and B_2O_3 are connected by interfaces, that occupy a considerable part of the total cell area. Thus the interface energy contributes strongly to the mixing energy. In the discussion above we showed that the mixing energy can easily be reduced by choosing larger unit cells with smaller interface-to-area ratios. In the thermodynamic limit the areas of the individual phases are large and the interface-to-area ratio tends to zero. In this case all data points with gray diamonds would be exactly on the convex hull, that is the Gibbs free energy of the compounds at zero temperature and zero pressure. This demonstrates that intermediate compositions of the 2D $B_{1-x}O_x$ binary system are heterogeneous mixtures of borophene and B_2O_3 .

Conclusion

In this work we used first principles calculations to study the compositional phase diagram of free-standing, two-dimensional $B_{1-x}O_x$ crystals for compositions ranging from $x = 0$ to $x = 0.6$, which correspond to borophene and B_2O_3 sheets, respectively. Our results show that the convex hull of the phase diagram is defined by borophene and B_2O_3 and no other phases. Intermediate compositions are thus heterogeneous mixtures of these two compounds. Hypothetical crystals with intermediate compositions such as B_2O ($x = 1/3$) are unstable, because their energies are significantly above the convex hull and some of them were found to undergo spontaneous disproportionation into borophene and B_2O_3 . This could explain why in the literature there are no conclusive reports about the existence of bulk B_2O . It is also found that oxidizing borophene inside the flakes is thermodynamically unfavorable over forming heterogeneous mixtures of borophene and B_2O_3 , fully consistent with previous reports on the tendency of borophene to oxidize from its edges (forming B_2O_3) rather than from the inside [4]. All findings can be rationalized by oxygen's preference of two-fold coordination which is incompatible with higher in-plane coordination numbers favored by boron.

These results are an important step forward to understand the oxidation behavior of 2D boron, which is crucial for its practical use in potential future electronic, optical or chemical applications. For future investigations it would be interesting to reconsider the compositional phase diagram on metal surfaces as in the experiment, which might be simplified by studying systems as a function of global charge transfer.

Acknowledgements

The work is financially supported by the German Research Foundation (DFG) under grant numbers SE 651/45-1. F.A. is financially supported by "Deutschlandstipendium". Computational resources for this project were provided by ZIH Dresden under project "nano-10". We thank Igor Baburin (TU Dresden) for helpful discussions.

Additional information

Supplementary material is available for this paper upon request by the authors. It contains the energies, compositions and structural illustration for all considered systems.

References

- [1] K. S. Novoselov, A. Mishchenko, A. Carvalho, and A. H. Castro Neto, *2D materials and van der Waals heterostructures*, Science. **353**, aac9439 (2016).
- [2] R. Mas-Balleste, C. Gomez-Navarro, J. Gomez-Herrero, and F. Zamora, *2D materials: to graphene and beyond*, Nanoscale **3**, 20 (2011).

- [3] A. J. Mannix *et al.*, *Synthesis of borophenes: Anisotropic, two-dimensional boron polymorphs*, Science **350**, 1513 (2015).
- [4] B. Feng *et al.*, *Experimental realization of two-dimensional boron sheets*, Nature Chem. **8**, 563 (2016).
- [5] I. Boustani, *New quasi-planar surfaces of bare boron*, Surf. Sci. **370**, 355 (1997).
- [6] J. Kunstmann and A. Quandt, *Broad boron sheets and boron nanotubes: an ab initio study of structural, electronic, and mechanical properties*, Phys. Rev. B **74**, 035413 (2006).
- [7] H. Tang and S. Ismail-Beigi, *Novel precursors for boron nanotubes: the competition of two-center and three-center bonding in boron sheets*, Phys. Rev. Lett. **99**, 115501 (2007).
- [8] X. Wu *et al.*, *Two-dimensional boron monolayer sheets*, ACS Nano **6**, 7443 (2012).
- [9] E. S. Penev, S. Bhowmick, A. Sadrzadeh, and B. I. Yakobson, *Polymorphism of two-dimensional boron*, Nano Lett. **12**, 2441 (2012).
- [10] Y. Liu, E. S. Penev, and B. I. Yakobson, *Probing the Synthesis of Two-Dimensional Boron by First-Principles Computations*, Angew. Chemie Int. Ed. **52**, 3156 (2013).
- [11] A. J. Mannix *et al.*, *Borophene as a prototype for synthetic 2D materials development*, Nat. Nanotechnol. **13**, 444 (2018).
- [12] D. Nieto-Sanz, P. Loubeyre, W. Crichton, and M. Mezouar, *X-ray study of the synthesis of boron oxides at high pressure: phase diagram and equation of state*, Phys. Rev. B **70**, 214108 (2004).
- [13] V. L. Solozhenko, O. O. Kurakevych, V. Z. Turkevich, and D. V. Turkevich, *Phase diagram of the B- B₂O₃ system at 5 GPa: Experimental and theoretical studies*, J. Phys. Chem. B **112**, 6683 (2008).
- [14] H. Dong *et al.*, *Boron oxides under pressure: Prediction of the hardest oxides*, Phys. Rev. B **98**, 174109 (2018).
- [15] K. Shirai, *Phase diagram of boron crystals*, Jpn. J. Appl. Phys. **56**, 05FA06 (2017).
- [16] H. Hubert *et al.*, *Icosahedral packing of B₁₂ icosahedra in boron suboxide (B₆O)*, Nature **391**, 376 (1998).
- [17] G. Ferlat, A. P. Seitsonen, M. Lazzeri, and F. Mauri, *Hidden polymorphs drive the vitrification in B₂O₃*, Nature Mater. **11**, 925 (2012).
- [18] G. Gurr, P. Montgomery, C. Knutson, and B. Gorres, *The crystal structure of trigonal diboron trioxide*, Acta Cryst. B **26**, 906 (1970).

- [19] C. Prewitt and R. Shannon, *Crystal structure of a high-pressure form of B_2O_3* , Acta Cryst. B **24**, 869 (1968).
- [20] H. T. Hall and L. A. Compton, *Group IV analogs and high pressure, high temperature synthesis of B_2O* , Inorg. Chem. **4**, 1213 (1965).
- [21] T. Endo, T. Sato, and M. Shimada, *High-pressure synthesis of B_2O with diamond-like structure*, J. Mater. Sci. Lett. **6**, 683 (1987).
- [22] M. P. Grumbach, O. F. Sankey, and P. F. McMillan, *Properties of B_2O : An unsymmetrical analog of carbon*, Phys. Rev. B **52**, 15807 (1995).
- [23] H. Hubert *et al.*, in *Mater. Res. Soc. Symp. - Proc.*, edited by R. Bormann *et al.* (Materials Research Society, , 1996), Vol. 410, pp. 191–196.
- [24] M. Daub and H. Hillebrecht, *Borosulfates $Cs_2B_2S_3O_{13}$, $Rb_4B_2S_4O_{17}$, and $A_3HB_4S_2O_{14}$ ($A = Rb, Cs$)—Crystalline Approximants for Vitreous B_2O_3 ?*, Eur. J. Inorg. Chem. **2015**, 4176 (2015).
- [25] P. Zhang and V. H. Crespi, *Theory of B_2O and $B_e B_2$ Nanotubes: New Semiconductors and Metals in One Dimension*, Phys. Rev. Lett. **89**, 056403 (2002).
- [26] C. Zhong *et al.*, *Two-dimensional honeycomb borophene oxide: strong anisotropy and nodal loop transformation*, Nanoscale **11**, 2468 (2019).
- [27] A. Lherbier, A. R. Botello-Méndez, and J.-C. Charlier, *Electronic and optical properties of pristine and oxidized borophene*, 2D Mater. **3**, 045006 (2016).
- [28] J. C. Alvarez-Quiceno, R. H. Miwa, G. M. Dalpian, and A. Fazzio, *Oxidation of free-standing and supported borophene*, 2D Mater. **4**, 025025 (2017).
- [29] R.-Y. Guo, T. Li, S.-E. Shi, and T.-H. Li, *Oxygen defects formation and optical identification in monolayer borophene*, Mater. Chem. Phys. **198**, 346 (2017).
- [30] Y. He *et al.*, *Tuning the electronic transport anisotropy in borophene via oxidation strategy*, Sci. China Technol. Sci. **62**, 799 (2019).
- [31] A. A. Kistanov, S. K. Khadiullin, S. V. Dmitriev, and E. A. Korznikova, *Effect of oxygen doping on the stability and band structure of borophene nanoribbons*, Chem. Phys. Lett. **728**, 53 (2019).
- [32] B. Feng *et al.*, *Dirac Fermions in Borophene*, Phys. Rev. Lett. **118**, 096401 (2017).
- [33] B. Feng *et al.*, *Discovery of 2D Anisotropic Dirac Cones*, Adv. Mater. **30**, 1704025 (2018).

- [34] W. Luo *et al.*, *The adsorption and dissociation of oxygen on Ag (111) supported chi 3 borophene*, Phys. B Condens. Matter **537**, 1 (2018).
- [35] R. Zhang, Z. Li, and J. Yang, *Two-Dimensional Stoichiometric Boron Oxides as a Versatile Platform for Electronic Structure Engineering*, J. Phys. Chem. Lett. **8**, 4347 (2017).
- [36] S. Lin *et al.*, *Porous hexagonal boron oxide monolayer with robust wide band gap: A computational study*, FlatChem **9**, 27 (2018).
- [37] T. Kambe *et al.*, *Solution Phase Mass Synthesis of 2D Atomic Layer with Hexagonal Boron Network*, J. Am. Chem. Soc. **141**, 12984 (2019).
- [38] J. M. Soler *et al.*, *The SIESTA method for ab initio order-N materials simulation*, J. Phys. Condens. Matter **14**, 2745 (2002).
- [39] N. Troullier and J. L. Martins, *Efficient pseudopotentials for plane-wave calculations*, Phys. Rev. B **43**, 1993 (1991).
- [40] J. P. Perdew, K. Burke, and M. Ernzerhof, *Generalized gradient approximation made simple*, Phys. Rev. Lett. **77**, 3865 (1996).
- [41] H. J. Monkhorst and J. D. Pack, *Special points for Brillouin-zone integrations*, Phys. Rev. B **13**, 5188 (1976).
- [42] K. C. Lau, R. Pati, R. Pandey, and A. C. Pineda, *First-principles study of the stability and electronic properties of sheets and nanotubes of elemental boron*, Chem. Phys. Lett. **418**, 549 (2006).
- [43] H. Remy, *Lehrb. der Anorg. Chemie Band 1* (Akademische Verlagsgesellschaft Geest & Portig, Leipzig, 1970), Chap. 10.